

Gradient core–shell HTS/polymer covered magnetoactive composites with ultrafine particles fabricated by 3D printing

I. Shishkovsky¹  · V. Scherbakov¹ · M. Kuznetsov²

Received: 28 July 2016 / Accepted: 4 October 2016 / Published online: 7 October 2016
© Springer Science+Business Media New York 2016

Abstract In this study, we report the laser synthesis and characterization of the core–shell high-temperature superconductor oxides of $\text{SrFe}_{12}\text{O}_{19}$ and CoFe_2O_4 phases covered with biocompatible polyetheretherketone shells of ultrafine particles and layerwise selective laser sintering of the 3D samples. The optimal regimes of such synthesis are being discussed. Optical and scan electron microscopy with EDX, X-ray diffraction studies show that both core–shell systems have a complex structure with interesting electro-physical properties. Expanding computer aid design of the HTS core distribution in polymer matrix opens door to manipulating the electromagnetic field distribution in such 3D complex core–shell samples.

Keywords Selective laser sintering (SLS) · High temperature superconductivity (HTS) · Core–shell structures · Polyetheretherketone (PEEK) · Electromagnetic field distribution

1 Introduction

The search and synthesis of new electro- and magneto- active materials are exhausted due to almost complete use of the existing chemical compositions and processes of their preparation in various solid states, and also due to limited functions of samples. Therefore

This article is part of the Topical Collection on Fundamentals of Laser Assisted Micro- and Nanotechnologies.

Guest edited by Eugene Avrutin, Vadim Veiko, Tigran Vartanyan and Andrey Belikov.

✉ I. Shishkovsky
shiv@fian.smr.ru

¹ Lebedev Physical Institute (LPI) of Russian Academy of Sciences, Samara Branch, Novo-Sadovaja St. 221, Samara, Russia 443011

² All-Russian Research Institute on Problems of Civil Defense and Emergencies of Emergency Control Ministry of Russia (EMERCOM), 7 Davidkovskaya Str., Moscow, Russia 121353

it is an urgent problem of today to switch over to multi-component mesoscopically inhomogeneous (i.e. functional graded, FG) meso- and nano- structures with different types of orderings (and different thermal, magnetic, piezoelectric, ferroelastic etc. properties—Shishkovsky 2011). Fundamentals of active elements fabrication from smart materials by the selective laser sintering/melting (SLS/M) method with a hybrid combination of some traditional processes were developed in our studies. Well known piezoelectric, hexaferrite and high-temperature superconductivity (HTS) systems [PbTi_{1-x}Zr_xO₃—named as PZT (Gureev et al. 2000); Li_{0.5}Fe_{2.52x}Cr_xO₄ and BaFe_{12-x}Cr_xO₁₉—spinel (Kuznetsov et al. 2006); YBa₂Cu₃O_{7-x}, NiFe₂O₄, CoFe₂O₄, SrFe₁₂O₁₉, Ni_{0.35}Zn_{0.65}Fe₂O₄—HTS (Kuznetsov et al. 2008)] were used for three dimensional (3D) active device printing.

In particular, porous materials based on the HTS can be practically ideal current limiters of short circuit, as far as, it being place, in the liquid nitrogen penetrating by pores, can bear critical currents, exceeding such for a solid HTS (Petrov and Tetueva 2003). At present time there are developed the new ways of materials and 3D parts manufacturing, one of which (for the case of HTS) can become the SLS/M method (Kuznetsov et al. 2008). Essential SLS advantage is a reduction of design time and making the product fabrication of any shape.

Radioabsorbing materials (RAM) are widely used for protection against electromagnetic fields (EMF), in particular, polymer composites with ferrimagnetic or ferromagnetic nano additives are used as RAM. Efficient RAM should satisfy a number of requirements: maximum absorption of electromagnetic waves within a wide frequency range, minimum reflection and lack of harmful fumes, fire safety, small dimensions, light weight and complex shape. So actual problem is development of an additive technology approach by composite manufacturing of magnetic polymer with inclusion of the HTS near sub micron particles for efficient screens defending from EM radiation of medical equipment, as well as from tissue hyperthermia of cancer. It is known that spinel ferrites and their composites effectively absorb EMR within the frequency band of 0.9–2.2 GHz. Hexagonal ferrites intensively absorb in the range of tens of GHz. So by combining the sub micron particles of magnetite and hexaferrites (e.g. strontium or cobalt hexaferrite) it is possible to improve the RAM performance at the edges of the frequency band, i.e. at few GHz and at tens GHz, thus significantly increasing the operating range of the RAM.

Earlier we have obtained the 3D parts from polymers (PA, PC etc.) with nano inclusions of magnetite and hematite phases (Shishkovsky et al. 2015). By the proposed method it is possible to fulfill polymer coatings with nanoparticles of the above mentioned ferrites on the surface of medical equipment thus providing its protective covering. At the present study, the near submicron particles of SrFe₁₂O₁₈ and CoFe₂O₄ were added to biocompatible polyetheretherketone (PEEK) powders for the layerwise SLS of the porous 3D parts. The optimal regimes for the HTS composite core/PEEK shell structures were determined. For the phase-structural examination of the 3D bio fabricated parts, the optical and scan electron microscopy with EDX, X-ray diffraction studies were used.

2 Materials and methods

The polyetheretherketone (PEEK—Vicatex Co., UK) was bought at the chemical market, and used as supplied. The size of the particles taken for the polymer fractions was 40–60 μm that was comparable with the laser beam diameter. It ensured a high stacking density of the particles in the initial metal-polymer composition (MPC) that resulted in its

qualitative sintering. The polymer was dried before mixing. The $\text{YBa}_2\text{Cu}_3\text{O}_{7-x}$, CoFe_2O_4 , $\text{SrFe}_{12}\text{O}_{19}$, $\text{Ni}_{0.35}\text{Zn}_{0.65}\text{Fe}_2\text{O}_4$, NiCr_2O_4 HTS phases were prepared in Institute of Structural Microkinetics and Material Sciences of RAS (Chernogolovka, Russia) by the self-propagated high-temperature synthesis method. They had near submicron sized particles ($\sim 2\text{--}5\ \mu\text{m}$) and were used as a filling material. Polymer mixtures with HTS particles were prepared in the following ratios by wt.: 20:1 and 10:1 (the first of the ratios is for the polymer). To achieve uniform compositions, the MPC was placed into a hermetically sealed container filled with metallic balls of different diameters (from 0.2 to 0.5 mm) and shaken during 6 h by a Czechoslovak “Chirana” vibrator.

A cw Nd^{+3} :YAG laser was used to carry out the SLS/M process. The beam power P ranged between 1 and 16 W. The laser beam scanned the powder mixture surface; and herewith the interval between laser beam passages ($70\ \mu\text{m}$) was close to the diameter of the laser beam. The optical facility used had a focal length of 147 mm and a 25-mm shift from the bottleneck. The layer-by-layer laser sintering process was performed in a specially designed camera under Ar or in air as described in our works early.

The structure of the sintered porous polymer matrices with incorporated HTS particles was studied by the optical microscopy (NEOTHOT 30 M, Carl Zeiss) and SEM (LEO 1450 microscope, Carl Zeiss) equipped with the EDX analysis (INCA ENERGY 300, Oxford Instruments). To examine the crystal structure of the submicron particles, the X-ray diffraction on a DRON-3 M powder diffractometer (Fe K_α radiation) was used. Their phase composition was determined using the JCPDS PDF data (PCPDFWIN ver. 2.02, release 1999) and Crystallographica SearchMatch ver. 3.102 program.

3 Results and discussion

The choice of the laser influence (LI) optimal regimes for sintering was made by means of the variation of the laser power P and scanning velocity V . Figure 1 shows results of the direct SLM of separate monolayers on the air. Oxygen of air is useful for stabilization of the HTS synthesis results. The HTS systems based on NiCr_2O_4 , NiFe_2O_4 oxides were flaked out after the SLS/M on small thin pieces. As it is seen, laser melting on air for $\text{YBa}_2\text{Cu}_3\text{O}_{7-x}$ and $\text{Ni}_{0.35}\text{Zn}_{0.65}\text{Fe}_2\text{O}_4$ oxides were to a certain extent successful. So we expected acceptable results for the layerwise direct SLM with these HTS oxide ceramics. The LI parameters that allowed obtaining solid (correct cube shape) samples without form buckling were considered optimal regimes.

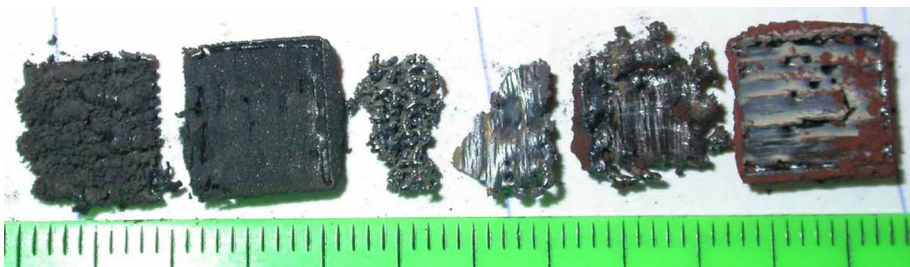


Fig. 1 Sintered monolayer appearance: from *left* to the *right*— $\text{YBa}_2\text{Cu}_3\text{O}_{7-x}$ (industrial and SHS), NiFe_2O_4 , CoFe_2O_4 , $\text{SrFe}_{12}\text{O}_{19}$, $\text{Ni}_{0.35}\text{Zn}_{0.65}\text{Fe}_2\text{O}_4$ —in air current. Regime of the LI was: laser power $P = 15.7\ \text{W}$, laser scan velocity $v = 1\ \text{cm/s}$

Figure 2 shows such successful attempts. During the layerwise synthesis each layer was processed twice. $\text{Ni}_{0.35}\text{Zn}_{0.65}\text{Fe}_2\text{O}_4$ oxide ceramics in spite of its “attractiveness” in monolayer regime, delaminated under layerwise SLS/M. The most acceptable results were achieved with the $\text{YBa}_2\text{Cu}_3\text{O}_{7-x}$ and $\text{SrFe}_{12}\text{O}_{19}$ HTS phases. Nevertheless, we could not consider these results (Fig. 2) successful because the shapes of samples were far from an ideal cube with a 10 mm corner. In the first case (Fig. 2a) the $\text{YBa}_2\text{Cu}_3\text{O}_{7-x}$ sample had great porosity and the $\text{SrFe}_{12}\text{O}_{19}$ sample (Fig. 2b) had significant shrinkage.

Based on our preliminary SLS/M results we proposed to use HTS ceramics with biopolymer mixtures. The optimal regimes for monolayer laser sintering were determined (Fig. 3). As it is seen from the plots in Fig. 3, the laser power growth leads to almost double rise of individual monolayer’s thickness.

The sintering quality was visually estimated by presence of carbonization traces (i.e., PEEK oxidative and thermal destruction) on the sintered surface as well as by the strength of adhesion between the sintered particles. The full PEEK destruction will obviously result in destruction of the relationships between the “skeleton” polymer particles and in nucleation of the three-dimensional (3D) sample crack. Argon environment in the synthesis chamber suppresses the polymer oxidative destruction. External appearance of separate monolayers (Fig. 4) has a more acceptable view in comparison with the direct SLM of the pure HTS powders (Fig. 1). Presented samples had elasticity and durability of PEEK matrix and can be recommended as RAM coatings in medical equipment after appropriate EM tests.

Moreover, these optimal regimes allowed us to fabricate the functionally graded 3D samples (Fig. 5a). As it is seen, CAD during the SLS/M allowed structure ordering of a magnetic component in the polymer mixture. The rationale for designing supermagnetic devices is the possibility of obtaining structures that can be manipulated in situ by applying external magnetic fields, which can also control specific processes at a cell level by releasing biomolecules and bioactive factors linked to magnetic nano carriers (Qiang et al. 2006; Riegler et al. 2013).

Figure 5b present lateral view of upper layers of the FG -Structure after SLS/M in PEEK + $\text{SrFe}_{12}\text{O}_{18}$ system under low magnification. We can clear register the gradient porous macrostructure of the 3D part.

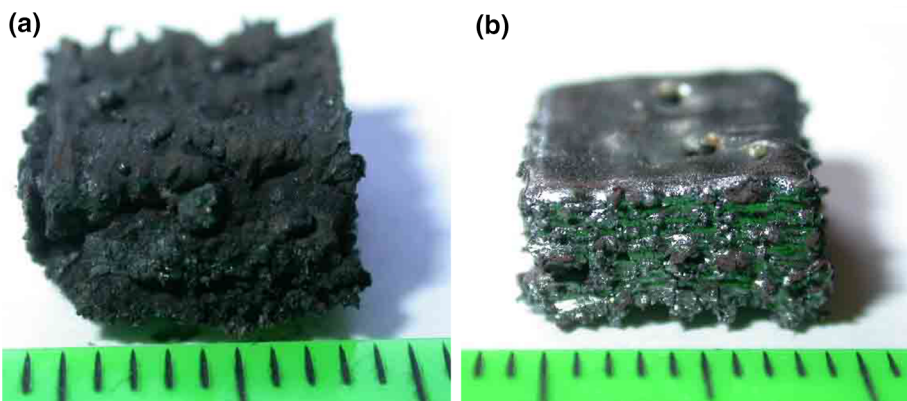


Fig. 2 3D parts were synthesized via direct SLS method: **a** $\text{YBa}_2\text{Cu}_3\text{O}_{7-x}$ and **b** $\text{SrFe}_{12}\text{O}_{19}$

Fig. 3 Sintered monolayer thickness as a function of the laser beam scanning speed: PEEK + SrFe₁₂O₁₈. *Dot line*— P = 1.6 W; *solid line*— P = 3.3 W

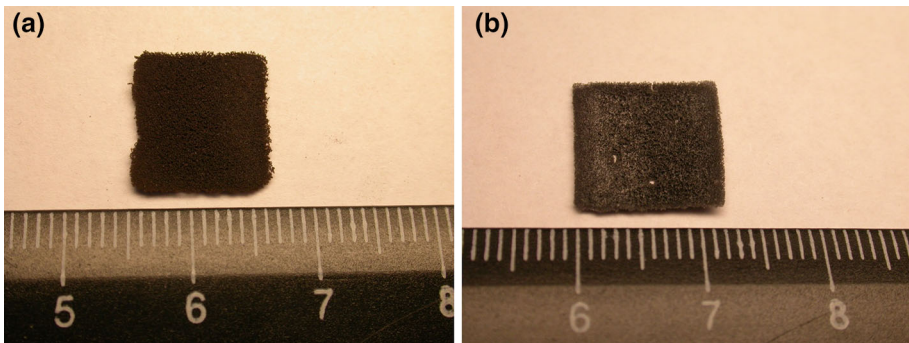
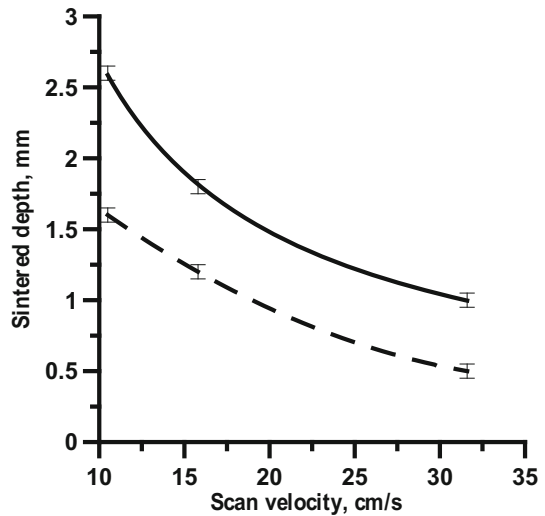


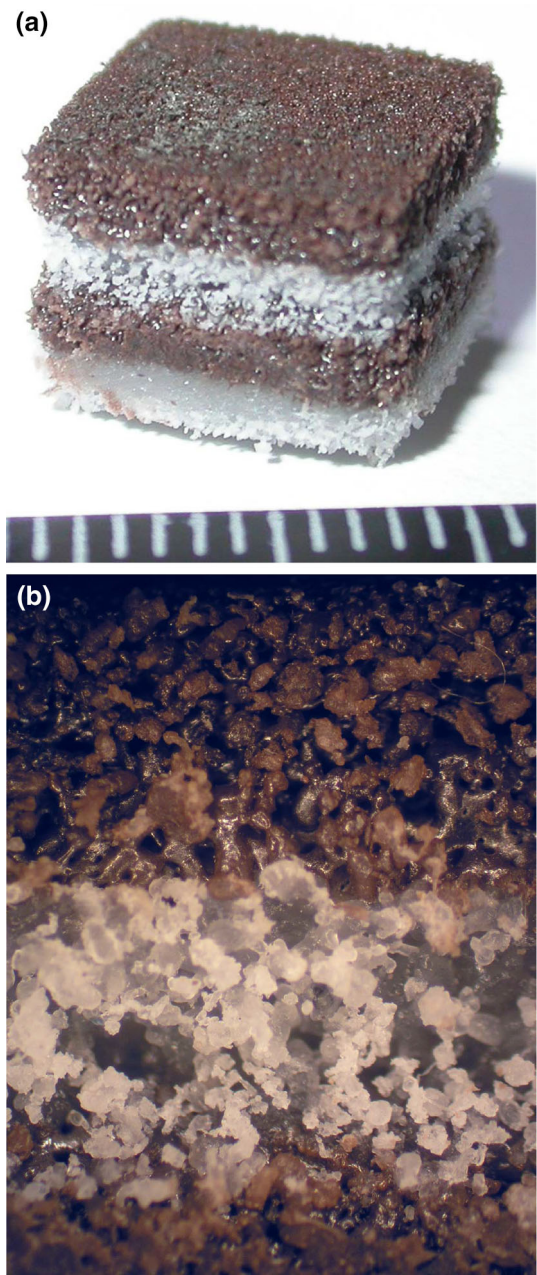
Fig. 4 Sintered monolayers appearance: **a** PEEK + SrFe₁₂O₁₉ = 10:1, P = 4 W, v = 9.4 cm/s; **b** PEEK + CoFe₂O₄ = 10:1, P = 2 W, v = 12.6 cm/s

The results of the optical metallography under high magnification for the sintered monolayers (Fig. 6) indicate, that the submicron HTS particles are incorporated into the polymer matrix (dark places stand for HTS particles and the lighter background is polymer) so we are dealing with the ensemble of magnetic multi-core particles. In contrast with the agglomerates of single-core particles (Qiang et al. 2006), the multi-core particles are assembled within a matrix that prevents further changes of the number of cores per particle in time.

These systems may present strong magnetic interactions between the cores as a result of their proximity to each other. Gutiérrez et al. (2015) noted that the number of magnetic cores per particle, their sizes, distances between them and their spatial distribution in general, all these parameters would strongly affect the magnetic properties of the material. In our opinion, the complexity of the problem of understanding the different magnetic properties of single-core and multi-core particles underlies the importance of reliable techniques for submicron particle synthesis capable of reproducing the particle size, shape and structural homogeneity, and also demands further researches.

Fig. 5 Overall view (a) of the sintered 3D functionally graded structures (10×10 mm by area) and lateral image (b) by optical microscopy (mag. $\times 25$):

PEEK + $\text{SrFe}_{12}\text{O}_{18}$ system;
 $P = 4.7$ W; $V = 15.8$ cm/s for PEEK layers and $P = 1.6$ W;
 $V = 15.8$ cm/s for $\text{SrFe}_{12}\text{O}_{18}$ layers. Through each five layers, the mixture composition is changed. *White color*—PEEK; *grey color*—the HTS additives



The X-ray diffraction patterns showed at the Fig. 7. The main reflections from strontium iron oxide— $\text{SrFe}_{12}\text{O}_{18}$ match with characteristic of the JCPDS card no. (33–1340) and main reflections from cobalt iron oxide— CoFe_2O_4 are equivalent to characteristic of the JCPDS card no. (79–1744). It should be mentioned, that the peak broadening due to the small core particle size throughout the series make the phase characterization still more

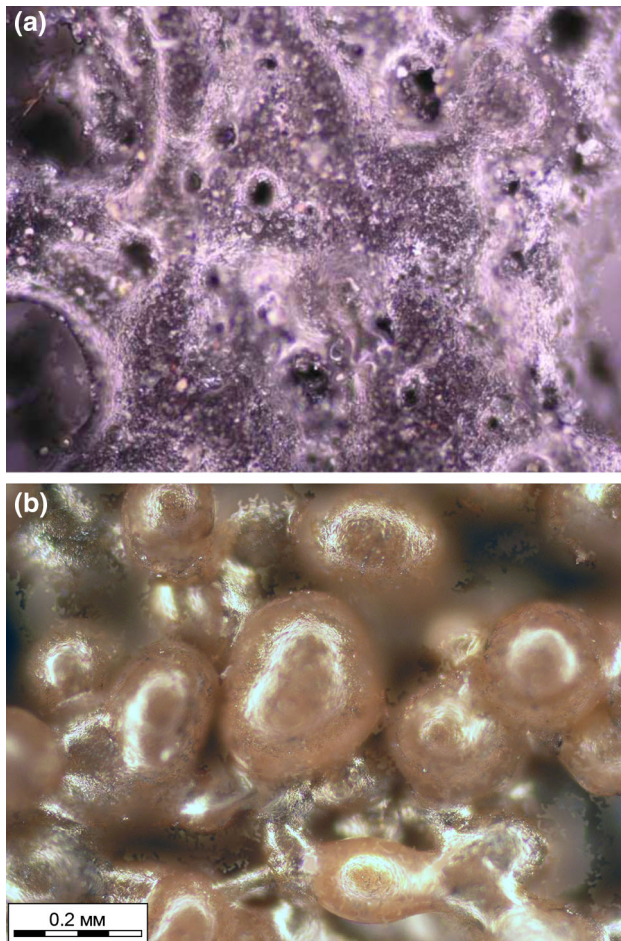


Fig. 6 Optical metallography of sintered macrostructures: **a** PEEK + CoFe_2O_4 system; **b** PEEK + $\text{SrFe}_{12}\text{O}_{19}$ system. The SLS regime, see above in Fig. 4; Magnification $\times 250$

complicated. Similar results we observed during the X-ray analysis for nano iron core/polymer shell structures (Shishkovsky et al. 2015). This can indicate of insignificant amount of the crystalline HTS oxides or other crystalline material formed. The large particles, even though they are few, make an important contribution to the diffraction patterns, since they contain a large fraction of the total number of atoms.

The SEM high magnification images for the monolayer surface of the PEEK + HTS are shown in Fig. 8a. The EDX microelement analysis (Fig. 8b) taken from the image regions confirms on the whole the initial $\text{SrFe}_{12}\text{O}_{18}$ oxides presence as well as the existence of the PEEK matrix. It should also be noted that in spite of the undesirable nanoparticles coagulation for nano oxides up to sub micron and micron sizes (Fig. 8a, b) promoted by laser heating, on the whole we observed that the nano-sized oxide crystals were well preserved.

Nevertheless, for everything mentioned above, we are of the opinion that the 3D rapid prototyped magnetic parts should be considered as a valuable candidate for the EMF

Fig. 7 X-ray diffraction patterns of the **a** PEEK + CoFe_2O_4 and **b** PEEK + $\text{SrFe}_{12}\text{O}_{19}$ systems

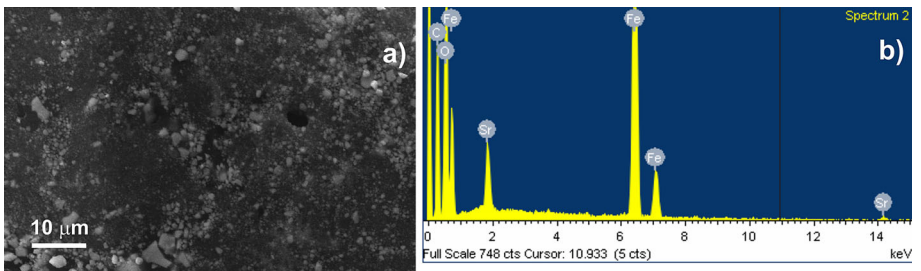
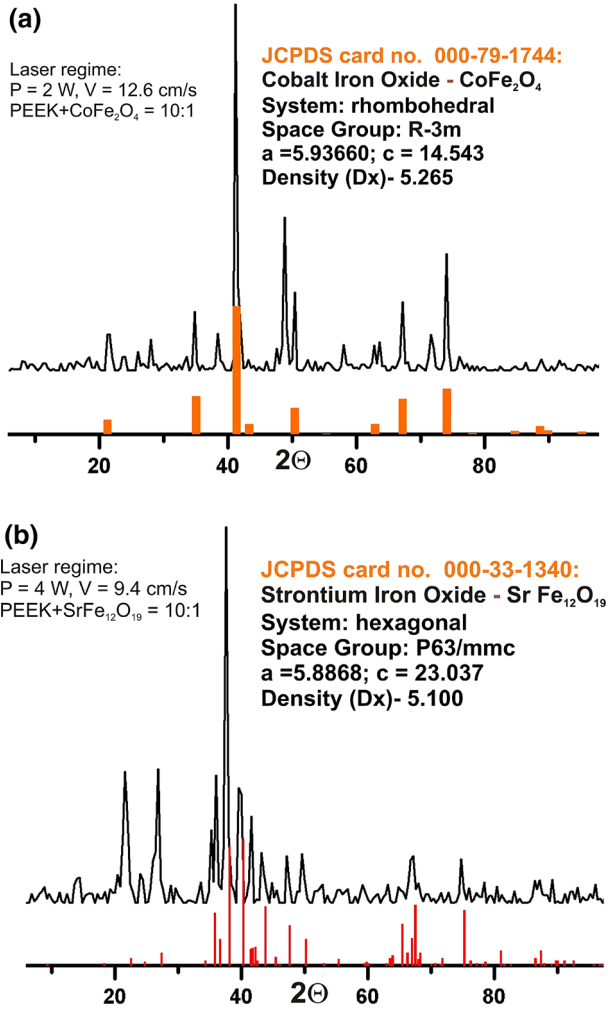


Fig. 8 High magnification SEM image with EDX analysis of the sintered surface for PEEK + $\text{SrFe}_{12}\text{O}_{18}$

absorber devices after corresponding metrological tests. Furthermore, a superparamagnetic scaffold (Russo et al. 2013) should provide a fascinating possibility to magnetically “switch” it on/off in order to deliver biofactors and stem cells, or to stimulate cell adhesion, proliferation and differentiation. At last, we can conclude that the SLS/M design of the 3D nanocomposite magnetic parts is characterized by a morphologically controlled structure (Fig. 5).

4 Conclusion

A principal feasibility for the fabrication of functionally graded 3D parts with near sub-micron HTS oxide particles, and for structural ordering was demonstrated and corresponding laser optimal regimes were determined. The SLS/M-fabricated 3D samples of biocompatible HTS core/PEEK shell magnetoactive composites have the potential to find medical application.

The possibility of association of several approaches (HTS oxides filler of PEEK) into a united technological process for layerwise syntheses of the FG- Structures and 3D parts with magnetic characteristics and with different types of ordering, were also shown. Mechanisms of formation of local zones of a specified configuration with magnetic characteristics during the melting (SLM/S) of submicron particles additives of transition metals with the HTS oxide ceramics in a polymer matrix were revealed.

Acknowledgments The study was supported by the grant of the Russian Science Foundation (Project no. 15-19-00208). Prof. M. Kuznetsov is separately grateful for financial support to the Russian Foundation of Basis Researches (Grant 13-03-12407 ofi-m2).

References

- Gureev, D.M., Ruzhechko, R.V., et al.: Selective laser sintering of PZT ceramic powders. *Tech. Phys. Lett.* **26**(3), 262–264 (2000). doi:[10.1134/1.1262811](https://doi.org/10.1134/1.1262811)
- Gutiérrez, L., Costo, R., et al.: Synthesis methods to prepare single- and multi-core iron oxide nanoparticles for biomedical applications. *Dalton Trans.* **44**, 2943–2952 (2015). doi:[10.1039/C4DT03013C](https://doi.org/10.1039/C4DT03013C)
- Kuznetsov, M.V., Parkin, I.P., et al.: Advanced ways and experimental methods in self-propagated high-temperature synthesis (SHS) of inorganic materials. *Mater. Sci. Forum* **518**, 181–188 (2006). doi:[10.4028/0-87849-405-7.181](https://doi.org/10.4028/0-87849-405-7.181)
- Kuznetsov, M.V., Shishkovsky, I.V., et al.: Design of 3D functional articles by combined SHS-SLS. *Mater. Manuf. Process.* **23**(6), 571–578 (2008). doi:[10.1080/10426910802160221](https://doi.org/10.1080/10426910802160221)
- Petrov, M.I., Tetueva, T.N., et al.: Synthesis, Microstructure, and the transport and magnetic properties of Bi-containing high-temperature superconductors with a porous structure. *Tech. Phys. Lett.* **29**(23), 986–988 (2003). doi:[10.1134/1.1639450](https://doi.org/10.1134/1.1639450)
- Qiang, Y., Antony, J., et al.: Iron/iron oxide core-shell nanoclusters for biomedical applications. *J. Nanoparticle Res.* **8**, 489–496 (2006). doi:[10.1007/s11051-005-9011-3](https://doi.org/10.1007/s11051-005-9011-3)
- Riegler, J., Liew, A., et al.: Superparamagnetic iron oxide nanoparticle targeting of MSCs in vascular injury. *Biomaterials* **34**, 1987–1994 (2013). doi:[10.1016/j.biomaterials.2012.11.040](https://doi.org/10.1016/j.biomaterials.2012.11.040)
- Russo, T., D’Amora, U., et al.: Systematic analysis of injectable materials and 3D rapid prototyped magnetic scaffolds: from CNS applications to soft and hard tissue repair/regeneration. *Procedia Eng.* **59**, 233–239 (2013). doi:[10.1016/j.proeng.2013.05.116](https://doi.org/10.1016/j.proeng.2013.05.116)
- Shishkovsky, I.V.: 3—Chemical and physical vapor deposition methods for nanocoatings. In: Woodhead Publishing Series in Metals and Surface Engineering, Woodhead Publishing, p 57–77. *Nanocoatings and Ultra-Thin Films*, ISBN 9781845698126. (2011). doi:[10.1533/9780857094902.1.57](https://doi.org/10.1533/9780857094902.1.57)
- Shishkovsky, I., Sherbakov, V., et al.: Layerwise laser-assisted sintering and some properties of iron oxide core/PEEK shell magnetic nanocomposites. *Microelectron. Eng.* **146**, 85–91 (2015). doi:[10.1016/j.mee.2015.04.030](https://doi.org/10.1016/j.mee.2015.04.030)